NAVAL POSTGRADUATE SCHOOL
Monterey, California

THESIS

AN INVESTIGATION OF
LASER INDUCED
SURFACE DAMAGE IN GLASS

by

Richard David Uyak

June 1985

Thesis Advisor: F. Schwirzke

Approved for public release; distribution is unlimited.

REPORT DOCUMENTATION PAGE

READ INSTRUCTIONS BEFORE COMPLETING FORM

1. REPORT NUMBER

2. GOVT ACCESSION NO.

3. RECIPIENT'S CATALOG NUMBER

4. TITLE (and Subtitle)
An Investigation of Laser Induced Surface Damage in Glass

5. TYPE OF REPORT & PERIOD COVERED
Master's Thesis
June 1985

6. PERFORMING ORG. REPORT NUMBER

7. AUTHOR(s)
Richard David Uyak

8. CONTRACT OR GRANT NUMBER(s)

9. PERFORMING ORGANIZATION NAME AND ADDRESS
Naval Postgraduate School
Monterey, California 93943-5100

10. PROGRAM ELEMENT, PROJECT, TASK AREA & WORK UNIT NUMBERS

11. CONTROLLING OFFICE NAME AND ADDRESS
Naval Postgraduate School
Monterey, California 93943-5100

12. REPORT DATE
June 1985

13. NUMBER OF PAGES
52

14. MONITORING AGENCY NAME & ADDRESS(if different from Controlling Office)

15. SECURITY CLASS. (of this report)

15a. DECLASSIFICATION/DOWNGRADING SCHEDULE

16. DISTRIBUTION STATEMENT (of this Report)
Approved for public release; distribution is unlimited.

17. DISTRIBUTION STATEMENT (of the abstract entered in Block 20, if different from Report)

18. SUPPLEMENTARY NOTES

19. KEY WORDS (Continue on reverse side if necessary and identify by block number)
Lasers; laser glass; plasma surface interactions; unipolar arcing; non-conducting materials; laser damage; plasma damage

20. ABSTRACT (Continue on reverse side if necessary and identify by block number)

Laser-induced plasma surface damage in a transparent dielectric is investigated. The possible occurrence of unipolar arcing as a damage mechanism in non-conductors is examined.

Experiments were conducted using a neodymium glass laser in a Q-switched mode to create a hot plasma. The plasma damage on both entrance and exit surfaces was examined. The morphology of damage is qualitatively analyzed. Several theories are applied in explanation of the damage obtained.

The appearance of micropitting at the periphery of the laser impact area of the targets indicates the possible occurrence of unipolar arcing as a damage mechanism. Other damage mechanisms include thermal stress, electron avalanche, particle deposition, and micropitting from particle inclusions or surface imperfections.

An Investigation of Laser Induced Surface Damage in Glass

by

Richard David Uyak
Lieutenant Commander, United States Navy
B.S., University of Akron, 1976

Submitted in partial fulfillment of the
requirements for the degree of

MASTER OF SCIENCE IN PHYSICS

from the

NAVAL POSTGRADUATE SCHOOL
June 1985

ABSTRACT

Laser-induced plasma surface damage in a transparent dielectric is investigated. The possible occurrence of unipolar arcing as a damage mechanism in non-conductors is examined.

Experiments were conducted using a neodymium glass laser in a Q-switched mode to create a hot plasma. The plasma damage on both entrance and exit surfaces was examined. The morphology of damage is qualitatively analyzed. Several theories are applied in explanation of the damage obtained.

The appearance of micropitting at the periphery of the laser impact area of the targets indicates the possible occurrence of unipolar arcing as a damage mechanism. Other damage mechanisms include thermal stress, electron avalanche, particle deposition, and micropitting from particle inclusions or surface imperfections.

TABLE OF CONTENTS

I. INTRODUCTION

In recent years, research into the development and application of high power lasers for both commercial and military uses has received much emphasis. The demands imposed on optical materials used in these laser systems has sparked much research into the prevention of damage to transparent dielectrics from high power laser pulses. Additionally, because of the expanding interest in the military uses of lasers, failure of glass as a target of laser pulses must be addressed. Solutions to these damage problems require a complete understanding of the damage mechanisms involved.

Damage to glass from high power laser pulses can be classified as either surface damage or bulk (internal) damage. By far the more serious of these is surface damage because surface damage occurs much more readily and at a lower laser intensity [Ref. 1]. Although surface damage can occur without the formation of a visible plasma [Ref. 2], all damage investigated here was caused by or accompanied plasma formation.

When a high power laser pulse is incident on a transparent dielectric, no visible damage occurs unless the energy of the pulse exceeds a certain minimum threshold value known as the damage threshold. Threshold studies have been made on a wide variety of glass targets and have indicated a material dependence on the condition of the surface of the glass (i.e., number of cracks, pores, or scratches); polishing techniques used in the production of the glass (etching or chemicals used); and any heavy metal ions embedded in the glass surface (either as a strengthener or as an unwanted result of the manufacturing process).

Additionally, the pulse length of the laser, the transverse mode of operation of the laser, and beam width of the pulse have been shown to affect the surface threshold. [Refs. 3-6]

Because the glass targets used are transparent and of finite size, two surfaces, the entrance (toward the laser) and exit (away from the laser), are affected by the laser pulse. The threshold for damage on the exit surface is less than that for the entrance surface creating an asymmetric damage pattern. This can be explained partly by the theory of Fresnel reflections [Ref. 7].

Many damage mechanisms are responsible for laser-induced glass damage. Among these are stimulated Brillouin scattering, thermal shock and resultant microplasma production caused by material defects or particle inclusions, electron avalanche at the surface, and thermal stress [Ref. 8]. The first of these is strictly an internal damage process and will not be discussed.

An electrical plasma surface interaction process that has been shown to be the primary cause of laser produced plasma damage to metal targets is unipolar arcing. Although demonstrated extensively in conducting surfaces, studies of unipolar arcing in non-conducting materials have been sparse. The theory of unipolar arcing does not limit laser damage to highly conducting materials. Part of the research presented here is to determine the extent of unipolar arcing in dielectric materials.

This thesis presents a qualitative description of laser-induced surface damage in glass and lays the framework for future study of the unipolar arcing process in poor conductors. Experimental results of numerous laser shots on glass slides are presented and analyzed.

II. THEORY

Damage to glass by laser pulses has received much attention in the scientific and industrial communities. Investigation of damage mechanisms has demonstrated the importance of a large number of factors in determining surface damage threshcldS. Scme of these variables include pulse-duration of the laser, beam diameter, beam focussing, laser transverse mode of operation, laser frequency, and details of target material preparation. This list becomes substantial when microscopic factors such as plasma formation parameters, heavy ion or dielectric particle inclusions, plasma instabilities, and thermal shock are considered. Many experimenters have failed to consider the importance of one or more of these parameters and, therefore, it becomes difficult to compare various experimental findings and to understand their relation to a particular damage theory. This chapter presents the theories relating to a number of possible damage mechanisms for surface damage in glass without specifying as to under what conditions one mechanism will dominate. The theories to be discussed are electron avalanche breakdown, absorption by impurity atoms, inclusions, or surface defects, Fresnel reflections, and unipolar arcing.

A. ELECTRON AVALANCHE BREAKDOWN

At high laser intensity levels, absorption of photons by atoms at the surface of the target material is sufficient to cause ionization and plasma formation. But those atoms not ionized or partially ionized may be excited by absorption of enough laser energy for the electrons to overcome the band

gap energy of the material. This produces an increased conduction band of electrons which can excite other electrons into the conduction band by impact ionization. Continuation of this process leads to an exponential increase in the number of conduction electrons. This process is called electron avalanche. [Ref. 9]

For electron avalanche to lead to breakdown of the material, the magnitude of the electric field must be sufficiently high for the duration of the pulse. This leads to the concept of a minimum electric field and associated laser power density at which breakdown occurs. Additionally, the lifetime of electrons in the conduction band must be large in comparison with the time between electron collisions in the avalanche chain. All this leads to a dependence on pulse duration for threshold level damage at energy densities on the order of 100 J/cm^2 or greater (Figure 2.1). For an energy density of 100 J/cm^2, the threshold is constant for pulse durations of about 10^{-7} seconds or less. Long pulses require a greater energy density to effect damage.

At high enough plasma temperatures, electron avalanche breakdown can occur away from the laser impact point in areas heated by the plasma alone. This usually requires some initiating mechanism for breakdown such as a "hot spot" created by a particle inclusion or surface defect. In fact the end result of hot plasma inclusion damage, discussed in the next section, is usually an avalanche breakdown of this type.

B. ABSORBING INCLUSIONS AND SURFACE DEFECTS

The initiation of electron avalanche damage is aided by local defects or inclusions at the laser impact area. The size of these inclusions or defects is usually much smaller than a wavelength [Ref. 10]. Any larger defects can usually

be detected before laser impact by optical inspection and therefore avoided.

1. Particle Inclusions

The mechanism of inclusion damage in glass is related to the temperature rise of particles or groups of particles near the surface relative to the surrounding glass [Ref. 11]. Metallic particles exhibit the greatest effect but at high enough temperatures, heating of ceramic or dielectric particles can also result in failure. A great many studies of platinum inclusions in laser glass have been made. The results of these can be extended to any metal or non-metal impurity.

As the laser-induced plasma expands and heats the surface, any particle inclusion or group of inclusions on or very near the surface will be heated. Metal inclusions will heat faster than the surrounding glass. The inclusion will expand according to its thermal expansivity and the glass-particle interface will be affected by the heat capacities and the thermal conductivities of both particle and glass. Temperatures of the particle can exceed 10^4K and a layer of molten glass may form around the particle [Ref. 6]. The expansion of the particle creates a stress in the nearby cooler glass which can be higher than the strength of the glass. This produces failure.

Many quantitative descriptions of this process have determined that the optimal radius of particles for damage to occur is on the order of 0.5 to 1.0 microns [Ref. 12]. This figure is pulse length dependent, however, as short laser pulses can more easily heat small inclusions and long pulses large inclusions [Ref. 8 :p. 13]. Damage can take many forms but usually consists of a small pit or crack in the surface which may have a spallation or microplasma ring around it.

2. Surface Defects

The surface of a glass can have many defects of microscopic size depending upon the care of manufacture, preparation, and handling. Figure 2.2 [Ref. 10 :p. 662] shows some representative glass surface defects. Referring to Figure 2.2, dimensions are r = 0.1 μm, c = 0.1 μm, and a = 1 μm. The electric field at these defects will be enhanced because of the build-up of standing waves inside the cavities. These electric field enhancements can be calculated by the application of electrostatics. The effect of the electric field enhancements is to concentrate more of the energy of the laser in the neighborhood of the cracks and pores so that the threshold for damage by electron avalanche breakdown may be increased by a factor of two to five depending on the geometry of the crack and dielectric constant of the material [Ref. 10 :pp. 661-662].

If absorbing particles are located near cracks or defects in the material, the increase in damage can be multiplicative. Microplasma production at these sites can occur because of the increased damage potential by evaporation and ionization of atoms heated by the large energy concentrations.

C. FRESNEL REFLECTIONS

One source of asymmetry that is present in surface damage experiments is wave reflection from the exit and entrance surfaces of glass. Figure 2.3 shows the electric field and wave vectors for a transverse polarized wave in air striking a thin glass target at normal incidence. The wave will be partially reflected at the entrance surface but the reflected wave will suffer a phase shift of 180° with respect to the incident wave because the glass has a higher index of refraction than air. Fresnel's equations give the

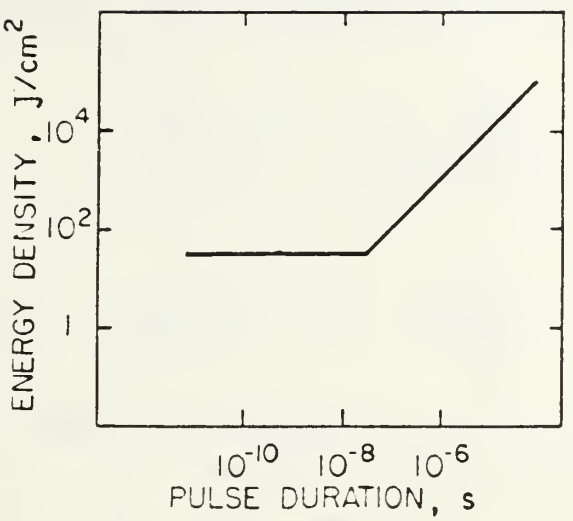

Figure 2.1 Electron Avalanche Damage Threshold.

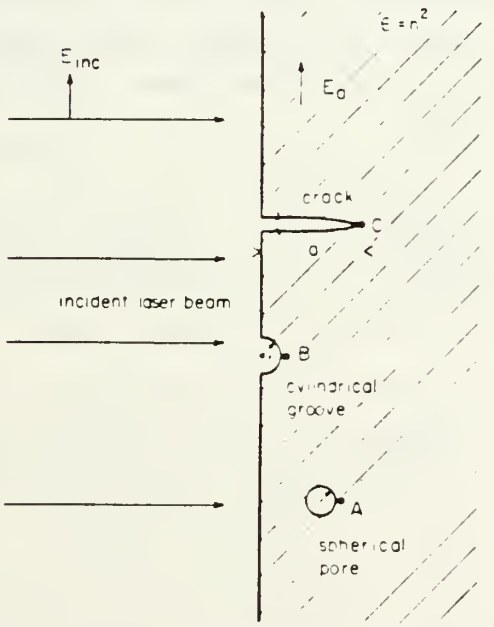

Figure 2.2 Typical Surface Defects in Glass.

relation between the magnitudes of the incident and reflected and the incident and transmitted oscillating electric field vectors at the surface of the glass as:

$$r_{ent} = \frac{E_{RI}}{E_I} = \frac{1 - n}{1 + n} \qquad (2.1)$$

$$t_{ent} = \frac{E_T}{E_I} = \frac{2}{1 + n} \qquad (2.2)$$

where E_I , E_{RI} and E_T are as depicted in Figure 2.3 and n is the index of refraction of the glass. r_{ent} is called the amplitude reflection coefficient and t_{ent} is called the amplitude transmission coefficient. For n = 1.5, an approximate value for glass, $E_T = \frac{4}{5} E_I$ or the electric field is reduced to four-fifths its incident value just inside the entrance surface. [Ref. 7 :p. 364]

At the exit surface, there is no phase shift of the incident wave so that the reflected wave increases the electric field vector across the interface. In this case, equations 2.1 and 2.2 become:

$$r_{ex} = \frac{E_{R2}}{E_T} = \frac{n - 1}{n + 1} \qquad (2.3)$$

$$t_{ex} = \frac{E_{exit}}{E_T} = \frac{2n}{n + 1} \qquad (2.4)$$

Then

$$E_{exit} = \frac{2n}{n + 1} E_T = \frac{4n}{(1 + n)^2} E_I \qquad (2.5)$$

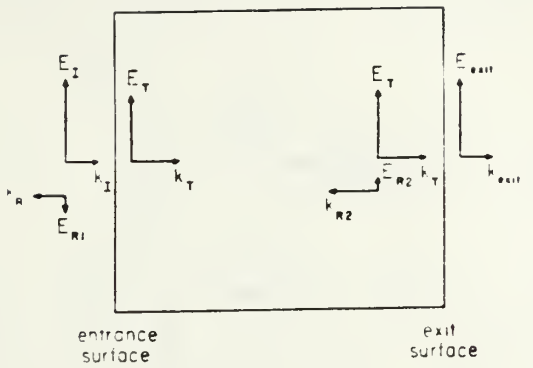

Figure 2.3 Electric Fields and Wave Vectors for a Tranverse Polarized Wave.

This amounts to 0.96 times the incident wave amplitude for an index of refraction of 1.5. The electric field at the exit interface maximizes because of the lack of phase shift of the reflected wave.

If the assumption is made that the amount of damage sustained by the glass is proportional to the amplitude of the electric field vectors, the above discussion leads to the conclusion that the damage at the exit surface of the material will be more severe than at the entrance surface. Experiments have confirmed this [Ref. 2 :p. 657].

Plasma formation on both entrance and exit surfaces affects the reflection and transmission of the incident wave at each surface. Figures 2.4 and 2.5 show exit and entrance surfaces respectively when a plasma is present. The index of refraction of a lossless plasma is given by:

$$n_p = \left(1 - \frac{\omega_p^2}{\omega^2}\right)^{1/2} \qquad (2.6)$$

where ω is the angular frequency of the incoming pulse and ω_p is the plasma frequency. The plasma frequency is given by:

$$\omega_p = \left(\frac{n_o e^2}{\epsilon_o m} \right)^{1/2} \qquad (2.7)$$

The plasma frequency is proportional to the square root of the free electron density so that as the density of the plasma changes the index of refraction will vary between zero and one. According to equations 2.6 and 2.7 , n_p is real as long as the plasma density is less than a critical density, n_c. When the plasma density exceeds this value, the index of refraction becomes imaginary. This leads to total reflection of the beam by the plasma. [Ref. 2 :p. 658]

As the plasma density increases, a standing wave is formed inside the glass near the exit surface. The electric field amplitude can increase quite dramatically within a quarter wavelength of the exit surface inside the glass leading to the potential for severe damage at the exit surface. The situation is reversed at the entrance surface for when the plasma density here increases past the critical density, the incident beam is reflected away from the glass. Thus the plasma shields the entrance surface from the beam. [Ref. 2 :p. 658]

The above descriptions do not take into account losses that occur in both the glass and the plasma which result in the heating of both. Very effective heating of the plasma leads to thermal shock and increased chance for damage by electron avalanche, inclusion stress, or unipolar arcing.

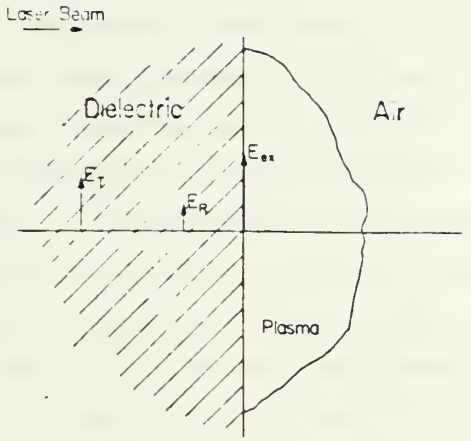

Figure 2.4 Exit Surface with Plasma Formation.

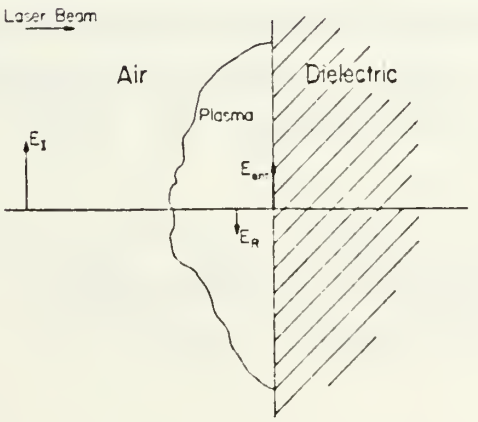

Figure 2.5 Entrance Surface with Plasma Formation.

D. UNIPOLAR ARCING

1. General

Unipolar arcing has been shown to be the primary plasma-surface interaction process when a laser-produced plasma is in contact with a conducting surface [Ref. 13]. Unipolar arcing is an electrical process which leads to crater formation when a sufficiently hot plasma is in contact with a wall. Many micro-arcs burn between the plasma and the wall driven by the sheath potential with the wall acting as both cathode and anode. [Ref. 14] provides a detailed description of the historical development of the theory of unipolar arcing.

According to the Robson-Thoneman model of unipolar arcing, for a unipolar arc to be sustained, the electron temperature, T_e, of the plasma must be high. The sheath potential, V_f, is established and depends on the electron temperature. Once an arc is initiated, the plasma potential then lowers to the cathode fall potential, V_c. An arc consists of a strong local emission of electrons from the cathode into the plasma. The plasma's quasi-neutrality must be maintained by a return electron current which reaches the surface through the lowered plasma potential and closes the current loop. The return current to the the plate of area A is given by:

$$I_c = A e n_e \left[\frac{kT_e}{2\pi m_e}\right]^{1/2} \left\{\exp\left(-\frac{eV_c}{kT_e}\right) - \exp\left(-\frac{eV_f}{kT_e}\right)\right\} \qquad (2.8)$$

where n_e is the electron density and e is the electron charge. The arc is sustained until I_c falls below a minimum value, I_a. The value of I_a depends upon the material of the plate [Ref. 15]. Figures 2.6 and 2.7 depict equilibrium flows between plasma and plate for this simple model.

The Robson-Thoneman model assumes a constant plasma density. The present Schwirzke-Taylor model for unipolar arcing [Ref. 15 :pp. 2-6] takes into account the fact that for an arc to develop, the ion density above the cathode spot must increase to allow for an increased electron flow to the plasma. This variation in plasma density increases the plasma pressure above the cathode spot which leads to an electric field component in the radial direction tangential to the surface. This radial field is given by:

$$E_r = - \frac{k T_e}{e n_e} \frac{d n_e}{d r} + \frac{j}{\sigma} \qquad (2.9)$$

where j is the current density and σ the electric conductivity. Figure 2.8 is a schematic of the Schwirzke-Taylor model.

2. Unipolar Arcing in Non-conducting Materials

Plasma-surface arcing is a dynamic process that must be described in terms of constantly changing variables. Some of these variables are plasma temperature and density, laser power and pulse duration, target surface material and properties such as electrical conductivity, vapor pressure as a function of surface temperature, and thermal conductivity.

Modifying equation 2.8 for an r-dependent electron flow to a ring area of $2\pi r \Delta r$ gives:

$$i^- = 2\pi r \Delta r\, n_e(r)\, e \left[\frac{k T_e}{2\pi m_e}\right]^{1/2} \exp\left\{-\frac{e}{k T_e}\left[V_p(r) - V_w(r)\right]\right\} \qquad (2.10)$$

where V_p (r) and V_w (r) are the plasma potential and the potential of the wall respectively. The sheath potential is then $V_s(r) = V_p(r) - V_w(r)$. The ion flow to the surface is determined by the number of ions entering the sheath and is independent of the sheath potential:

$$i_s^+ = 0.4\, e\, n_i(r) \left[\frac{2 k T_e}{M_1}\right] 2\pi r \Delta r \qquad (2.11)$$

The surface will be charged with a net charge when i_s^+ and i^- differ. Since $n_e(r) = n_i(r)$, the exponential term of equation 2.10 will largely determine the net surface charge. As seen in Figure 2.8, the plasma potential decreases with increasing radial distance from the crater such that the surface charge becomes more negative away from the cathode spot. This sets up a surface electric field with the cathode spot more positive than the surrounding ring area. The return current will then depend on the electron surface mobility and diffusion. [Ref. 15 :p. 8]

For a material of high resistivity to initiate and sustain an arc, electron surface mobility must be high enough for this return current to complete the current loop. At the high plasma temperatures known to occur on the order of 10^4K in glass [Ref. 7 :p. 655], thermal breakdown at the surface of the glass can lead to liberation of electrons and

vaporization of atoms from the material. This becomes more significant at surface irregularities or heavy ion inclusion spots (see sections A and B above). Actual dielectric breakdown of the glass can occur in localized spots which allows a flow of current to be set up. If conditions like this exist, which becomes likely at high enough plasma temperatures, an arc can be initiated and sustained long enough for a crater to form. However, it is logical to conclude that the size of the crater thus formed will be smaller than one formed in conducting materials. Schwirzke [Ref. 15 :p. 12] describes the results of experiments to determine the effect of laser pulses on conducting materials coated with a non-conducting coating and semi-conducting silicon. The results indicate that unipolar arcing does occur in these materials but that the sizes of the craters are smaller than in conducting materials. Although the degree of conductivity of the materials in Schwirzke's work is still orders of magnitude greater than that of glass, the instabilities and non-uniformities associated with a high energy laser produced plasma interfacing with a surface can be expected to greatly influence properties such as conductivity. The theory of unipolar arcing needs further refinement as investigation of the effects of high temperature plasmas proceeds.

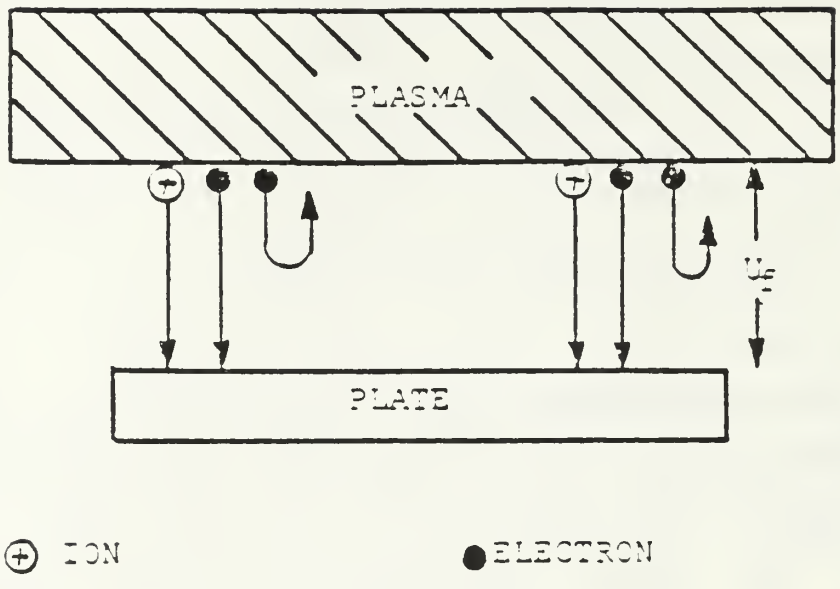

Figure 2.6 Equilibrium of Isolated Plate with no cathode spot.

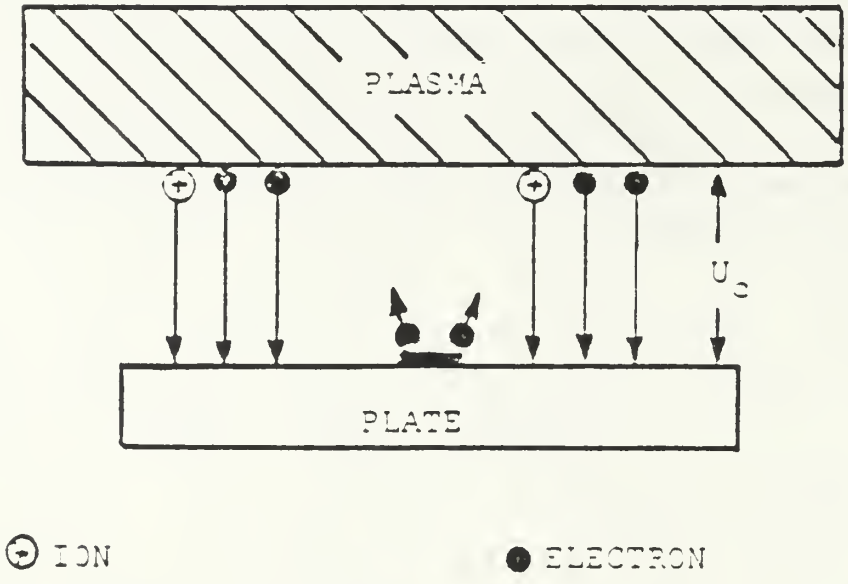

Figure 2.7 Equilibrium of Isolated Plate with a cathode spot.

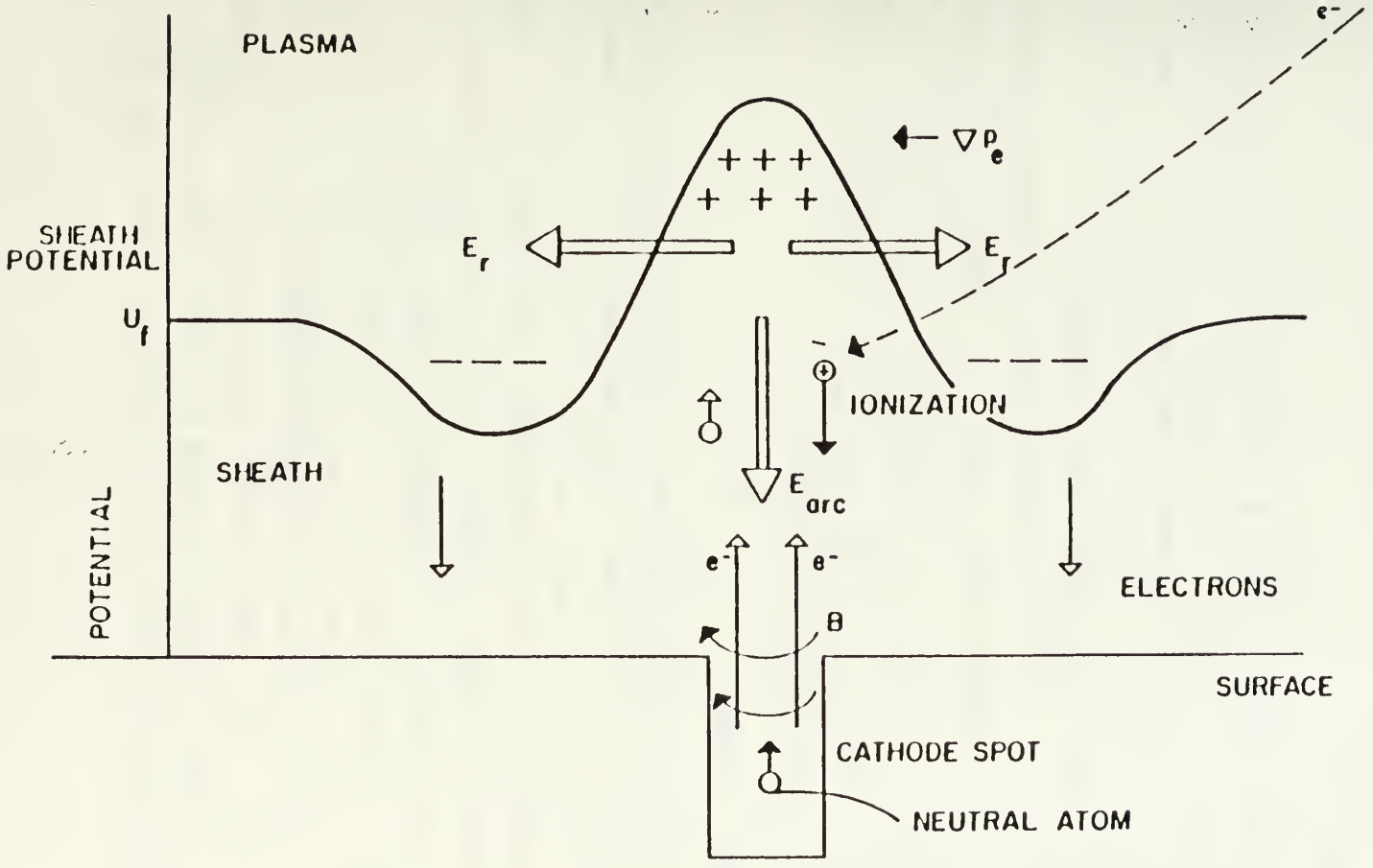

Figure 2.8 Unipolar Arc Model.

III. EXPERIMENTAL DESIGN

A. EQUIPMENT

The equipment used in this thesis consists of a neodymium glass laser and target test chamber. An optical microscope and a scanning electron microscope were used to evaluate target damage. Figure 3.1 shows the experimental set-up of the laser and target test chamber.

The laser was used to irradiate test samples placed in the target test chamber under vacuum. Samples were evaluated for surface damage by examination under optical and scanning electron microscopes. Polaroid photographs taken of the laser interaction with the target surface were used to verify the existence of a plasma.

1. Laser System

A KORAD K-1500 Q-switched neodymium glass laser was used to irradiate the target surfaces and form the damaging plasmas. This laser emits nominal 25 nanosecond (FWHM) pulses of wavelength 1.06 micrometers with a variable energy output of between 1 and joules. A detailed description of the laser installation is provided in [Ref. 16].

The incident laser pulse was highly focussed on the target to an impact area of from roughly 0.3 to 4.0 x 10^{-3} cm^2 giving an irradiance on target of from 0.75 to 16.5 kilojcules/cm^2. The laser total output energy was measured through an 8% beam splitter using a Laser Precision RK-3200 Series Pyroelectric Energy Meter reading from an RE 549 detector.

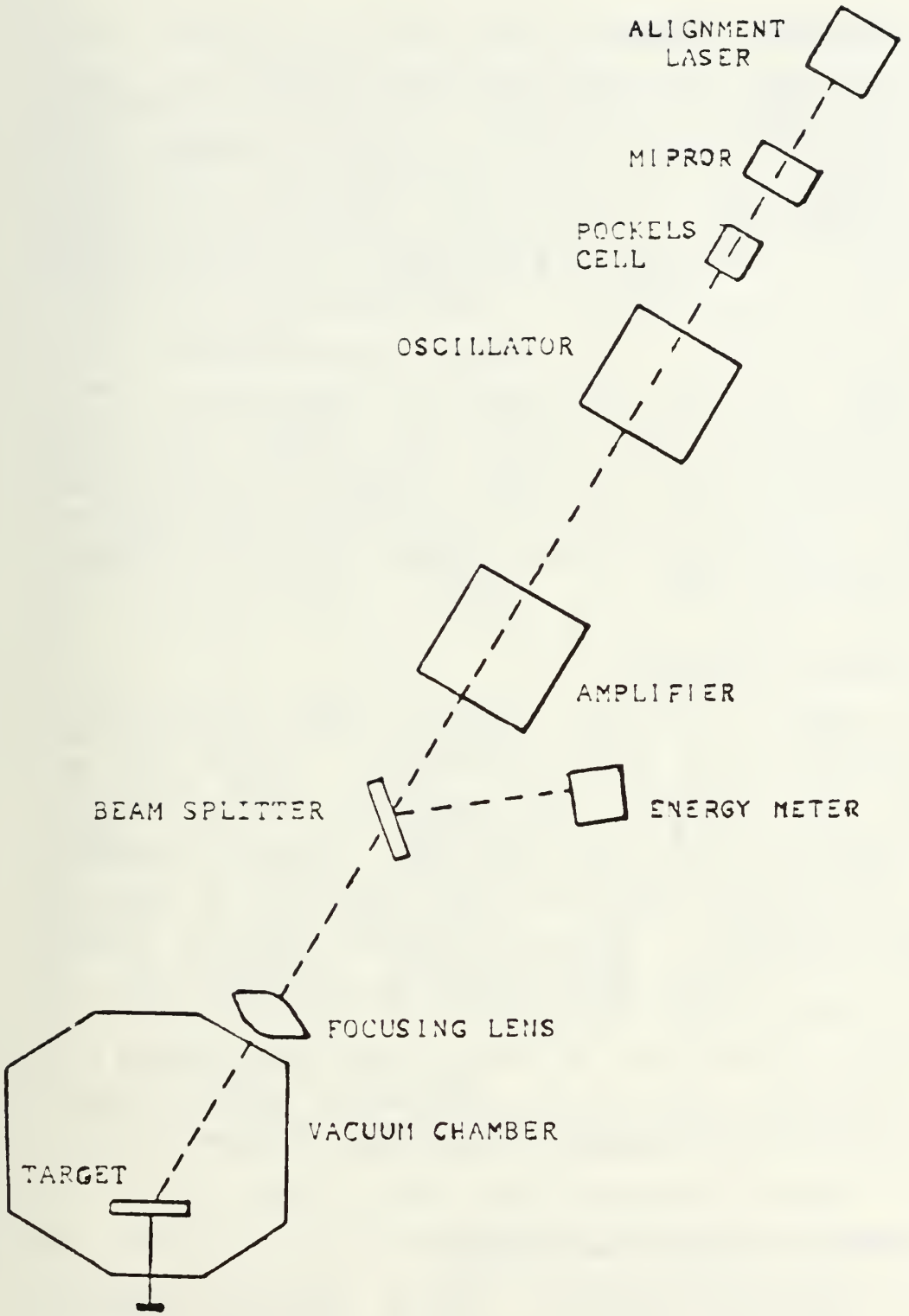

Figure 3.1 Laser and Target Test Chamber Arrangement.

2. Target Test Chamber

The target test chamber is a polyhedron of unbaked aluminum with an internal volume of 12.9 ± 0.3 liters. The vacuum system, using an oil diffusion pump and liquid nitrogen cooled baffle, can provide pressures of the order of 10^{-6} Torr. The laser beam was aligned 30 degrees from normal to the target surface. The targets were held by a probe holder inserted in the chamber through a vacuum seal. A lens holder in front of the chamber allows the placement of a focussing lens. Two different focal length lenses were used, a 30.0 cm and a 19.4 cm lens. The distance from lens to target was varied from 26.0 cm to 30.0 cm. An observation port on top of the chamber allows access for photography of the laser shots.

3. Optical Microscope

A Bausch and Lomb Dynazoom Bench Metallograph optical microscope was used to examine the target surfaces before and after damage. The Bausch and Lomb microscope provides magnifications from 50 to 800X. A photo attachment assembly to the microscope allows photographs to be taken of the target samples. This microscope utilizes direct lighting of the target samples through the lens but, by using an outside light source directed on the target, a greater depth of field can be seen. Indirect lighting was used by itself or with direct lighting to give a better overall perspective of target damage than direct lighting alone.

4. Scanning Electron Microscope

A Cambridge Stereoscan S4-10 Scanning Electron Microscope (SEM) was used to examine some of the targets. In order for the targets to be seen with the SEM, they were

first coated with a thin layer of either aluminum or gold in order to provide a conducting surface to act as the electron collector in the SEM. A VEECC VE-401 Automatic High Vacuum Evaporator was used for this purpose. The SEM provides magnifications from 20 to 100,000X. The advantage of the SEM is that it can provide higher magnifications and greater depth of field at lower magnifications.

5. Targets

The targets for the laser shots were Corning Micro Slides, no. 2947, 3 x 1" plain, thickness 0.96 to 1.06 mm, manufactured for general laboratory usage. They were chosen as target samples because of their availability, cost, and generally consistent content. The glass of these slides is an ordinary soda-lime window glass, lower in iron than typical window glasses. The iron content of the glass, a by-product of manufacturing, expressed as Fe_2O_3, is 0.03%. The approximate composition of the glass is: Silica (SiO_2) - 72%, Soda (Na_2O) - 15%, Lime (CaO) - 9%, Magnesium Oxide (MgO) - 3%, and Aluminum Oxide (Al_2O_3) - 1%. Table I contains selected properties of this particular glass. Chapter II of this thesis contains information on the effects of some of these properties on the damage resistance of this glass to laser pulses. [Ref. 17]

B. EXPERIMENTAL PROCEDURE

1. Sample Preparation and Target Shots

The glass slides were thoroughly cleaned with soap and water, then with acetone and methyl alcohol before being mounted in the test chamber. One slide was not cleaned at all before mounting in order to compare the degree of damage with the degree of surface contamination. Selected samples were then examined under the optical microscope using both

TABLE I

Selected Properties of Target Glass

Type	Soda Lime
Color	Clear
Thermal Expansion	0-300°C: 93.5 X 10^{-7} cm/cm-°C
Thermal Stress Resistance	16°C
Density	2.47 g/cm^3
Young's Modulus	7.1 X10^3 kg/mm^2
Log_{10} of Volume Resistivity (ohm-cm)	25°C: 12.4 250°C: 6.4 350°C: 5.1
Dielectric Constant	7.2 at 1 MHz, 20°C
Refractive Index	1.512 (at 589.3 nm)

Source:
[Ref. 17 :pp. 8-9]

direct and indirect lighting to test for cleanliness and inspect the surface for any apparent defects. Once placed in the chamber, the vacuum system was activated and the chamber was pumped down to a pressure of 10^{-6} Torr or less. A Helium-Neon laser was used to align the target at the correct position in the chamber. The correct lens was placed in the lens holder and then the distance from lens to target was measured.

The laser was fired at the target while a Polaroid snapshot of the impact was made to verify the existence of a plasma. Shots without apparent plasmas were disregarded and new slides were inserted as targets. The old slides were discarded. The energies of the shots were read off the energy meter and recorded.

2. Surface Damage Investigation

The damaged samples were thoroughly examined under the optical microscope on both the entrance and exit surfaces. Selected samples were then coated with aluminum or gold in the evaporator and mounted for viewing under the scanning electron microscope. The samples were then examined with the SEM.

IV. RESULTS

Numerous laser shots were made on 1.0 mm thick glass slides at different focal distances and varying power densities. The main types of surface damage observed can be classified into five categories: 1) large exit surface pitting, 2) entrance surface cracking or crazing, 3) rippling or melting of the surface at the impact area, 4) ring formation, and 5) micropitting caused by particle inclusions or by imperfections in the surface. Not all of these damage results occurred in every case, but rather the power density of the laser on the target affected the type and degree of damage encountered.

Small (on the order of 1 micron) diameter holes have also been observed and photographed which could possibly be unipolar arc craters. These holes exist to a varying degree in all targets and have somewhat the characteristic appearance of unipolar arc craters. Unipolar arcing is discussed following a detailed description of the other damage mechanisms below.

A. PLASMA SURFACE DAMAGE

1. Large Exit Surface Pitting

Large pits in the exit surface of the 1.0 mm thick glass targets were observed in several shots. In each case, the slide was situated at or near the focal point of the lens in the target test chamber. Figure 4.1 shows one such pit of an approximate diameter of 1.2 mm. The shot that produced this damage had a power density of 694.4 gigawatts/cm^2 and energy density of about 16.2 kilojcules/cm^2, a value much much greater than the threshold

level of about 110 joules/cm² [Ref. 5 :p. 53]. The depth of the crater is approximately 0.6 mm or one-half the diameter. Surrounding the crater appear to be tracks of material ejected from the crater radially and deposited on the glass surface. These tracks extend outwards 0.8 mm from the edge of the crater fairly symmetrically. Although a plasma was present on the exit surface and helped cause damage, the ring formation normally seem for plasma surface interactions (see subsection 4 below) is not observed outside the crater. This indicates that the plasma cloud may not have extended beyond the rim of the crater. The observed pattern is analogous to an explosion where particles are spewn out from the center in all directions. Those with the greatest momenta will be deposited farthest from the crater. The fractured appearance of the crater suggests such an explosion has taken place on or very near the surface of the glass.

The explanation of the crater formation itself follows from Fresnel reflection theory. A large amplitude standing wave is created inside the glass within a quarter wavelength of the exit surface. This large amplitude E field initiates pitting. As the pit forms, absorption of the beam is enhanced by the irregular surface of the pit and the size of the pit increases dramatically for the length of the pulse as material is ejected outwards at high velocities from the surface [Ref. 15 :pp. 655-660].

2. Entrance Surface Cracking

In all cases in which large exit surface pitting occurred, the entrance surfaces were damaged much less severely. Figure 4.2 is a photograph of the entrance surface of the same target as Figure 4.1 . No pitting has occurred but rather a cracking or crazing of the surface is apparent. Additionally, a rippling of the surface has

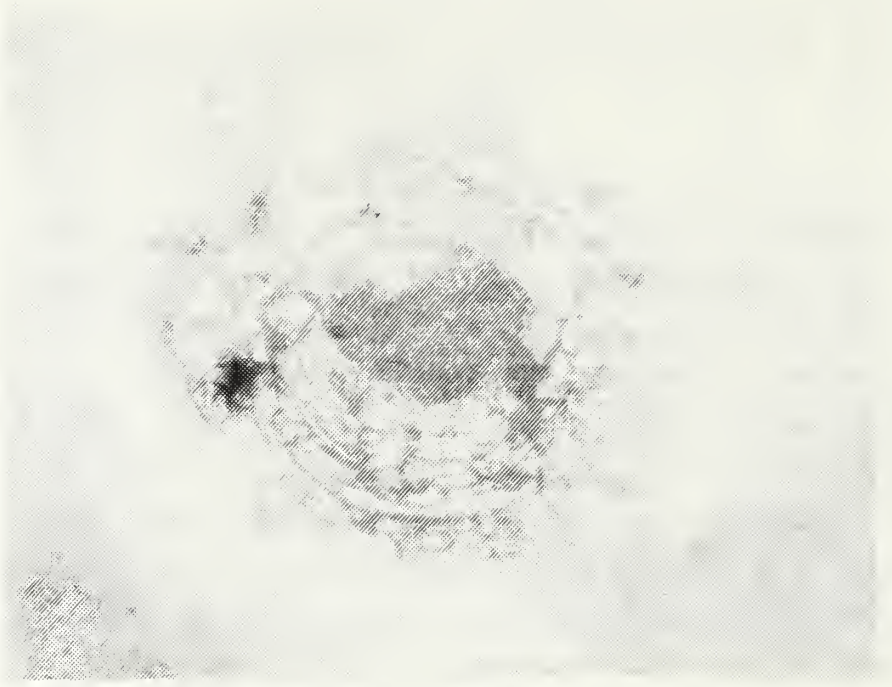

Figure 4.1 Large Exit Surface Crater, 1.2 mm diameter (50X Optical).

Figure 4.2 Entrance Surface Cracking (50X Optical).

occurred in areas where the cracking has not. The surface rippling is centered at the laser impact area and the cracks extend in almost all directions from there. The damage observed in Figure 4.2 is apparently caused by thermal stress as the hot, expanding plasma interacts with the target surface. The entrance surface plasma is hotter than the exit surface plasma [Ref. 15 :pp. 655-660] which may explain why cracking was never observed on the exit surface of targets. The fact that no pitting occurs at the entrance surface indicates that the damage on this surface is caused by the plasma, that is, external to the surface and not by any factors internal to the glass. This contrasts with the large exit surface pitting damage which indicates an internal mechanism for damage. Because glass is a non-crystalline material with no regular internal structure, the non-uniform appearance of the cracks is as predicted.

3. Surface Melting

The deformation of the glass at the laser impact point of Figure 4.2 is a rippling of the surface caused by melting and upheaval of the glass. This thermal stress was seen to occur on most target shots. The plasma created is quite hot initially, on the order of 10^4K or greater [Ref. 15 :p. 655]. The characteristic time for plasma formation is on the order of one nanosecond [Ref. 18], so that as the plasma grows and expands, it shields the surface from the remainder of the laser pulse. Thus the plasma absorbs a great deal of the laser energy and the result is thermal shock to the surface. This effects the rippled deformation and the cracking of the surface.

Figure 4.3 is a photograph of a laser impact area on the entrance surface of a target sample. The power density of this laser shot was 59.4 GW/cm^2 at an energy density of 1485.4 J/cm^2. The laser was focussed at a point 6.6 cm in

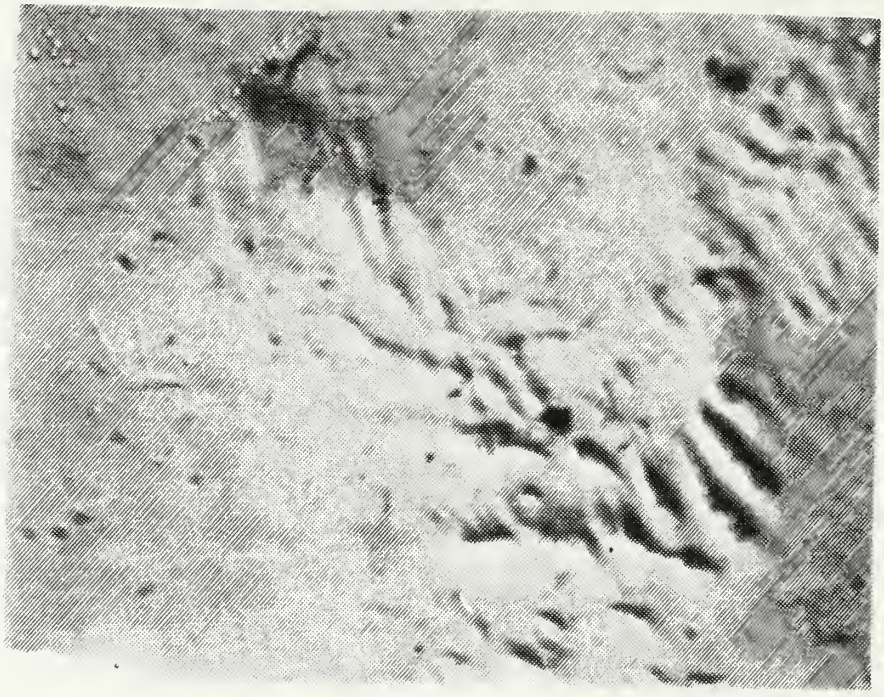

Figure 4.3 Entrance Surface Deformation (200X Optical).

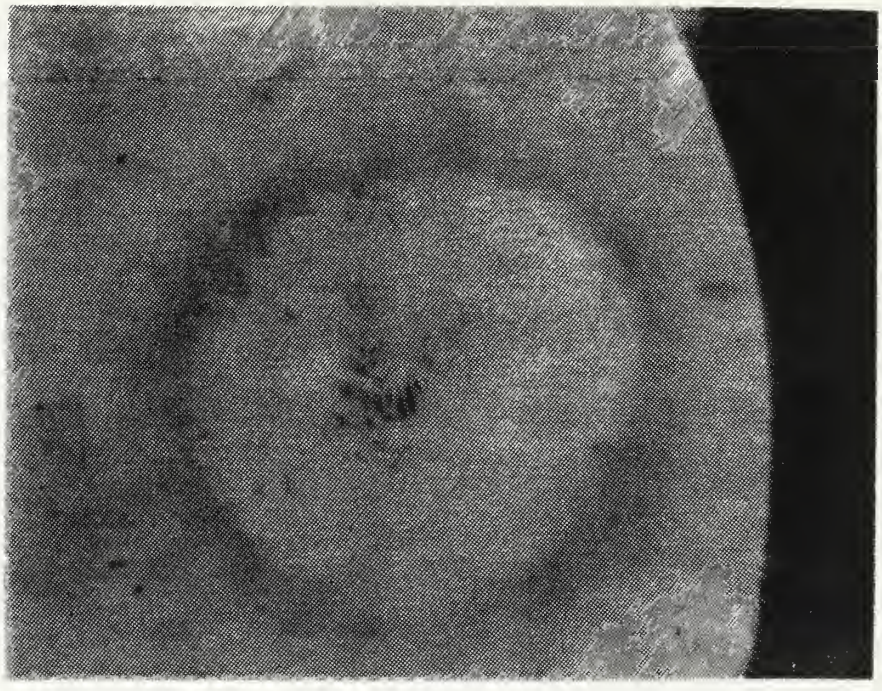

Figure 4.4 Ring Formation (50X Optical).

front of the target surface and thus the beam size at the front surface of the target was much smaller than at the exit surface. This created a greater damage pattern on the front surface than cn the back in contrast to the normal damage pattern. No pitting of either surface was cbserved even though the power density on target was large. The photograph of Figure 4.3 was taken utilizing offset background illumination to provide a greater depth of field. Note the series of parallel ridges, the longest of which is about 75 microns long. The melted portion of the target encompassed a diameter of about 0.4 mm. The area at the bottcm right of the photograph has a much more rippled appearance due to the radial asymmetry of the laser pulse and the 30° offset from normal incidence of the beam striking the target.

4. Ring Formatiçn

Figure 4.4 is a lower magnification of Figure 4.3 showing the ring structure that was the most frequently cbserved damage pattern in glass target shots. This ring has an inner diameter of 1.2 mm and an outer diameter of 1.8 mm. The ring is ccmposed of particles deposited on the glass that can not be washed off with acetone or methyl alcohcl. Ring structures were observed to occur in all laser shcts of lower power density on the entrance surfaces of the targets and sometimes on the exit surfaces. The sizes of the rings varied with power density, the larger rings occurring at greater power levels. The ring structure of Figure 4.4 has at least four noticable concentric rings formed. Figure 4.5 is a close-up of a different ring structure consisting of two outer rings with at least one inner ring. The structure of the rings has an orange peel appearance at higher magnifications clearly showing the deposited material on the surface.

The size of the rings was always seen to be larger than the size of the damaging beam indicating that the ring damage was caused by the plasma and not by the laser pulse itself. A possible explanation of the ring formation is as follows. The initial plasma is formed in the area of the melted surface at a temperature of roughly 10^4K. The hot plasma expands over the surface while still acquiring more energy from the pulse at its center. As the plasma expands and contacts the glass surface, it cools and the plasma begins to condense. Thus the outer edge of the ring structure, according to this explanation, should mark the limit of plasma surface damage. This is consistent with the experimental evidence that indicates no damage beyond the outer ring. It was once thought that the different rings were formed by different components of the plasma condensing out at different temperatures. However, Boling and Dube [Ref. 19], now believe that mode beating of the laser pulse "drives" the plasma so that the plasma temperature follows the power peaks on the pulse. The radius of a particular ring then depends on the temperature of the plasma in its beginning stage. The temperature in this stage is in turn a function of the laser beam power absorbed by the plasma.

Another possible explanation of the ring formation follows from studies of laser-produced plasma clouds. Radial bouncing of the plasma was seen to occur where the plasma comes to rest momentarily at the bounce radius, that is, at the turning point, and then is accelerated back. While stopped momentarily, the plasma deposits some of its material in the form of a ring. [Ref. 20]

Figure 4.5 shows spikes of deposited material pointed toward the center of the laser shot. This could possibly be caused by cooler spots at the front of the plasma. The inner edge of the rings was found to be an area where micropitting and arcing frequently occurred.

Figure 4.5 Ring Formation (200X Optical).

Figure 4.6 Ring Structure Showing Micropit at Center (200X Optical).

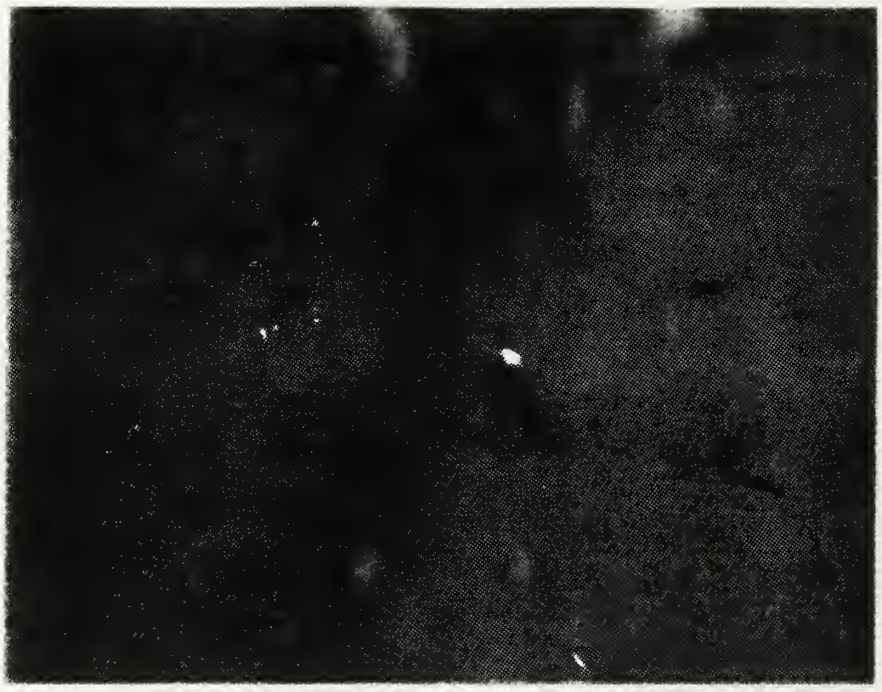

Figure 4.7 Ring Structure Showing Large Micropit at Periphery (200X Optical).

Figure 4.8 Micropit at Center of Ring Structure (400X Optical).

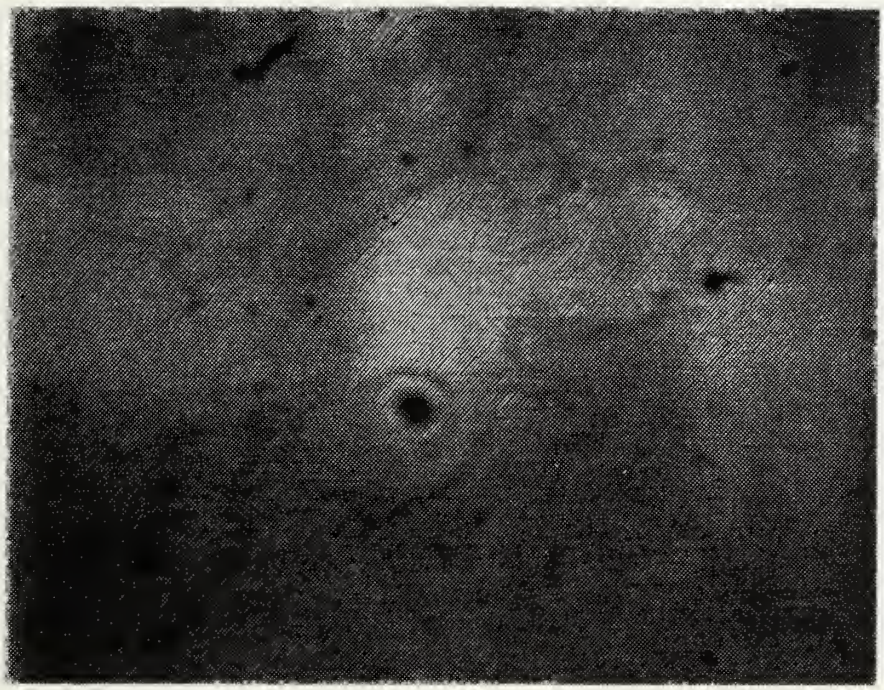

Figure 4.9 Micropit of Figure 4.8 (800X Optical).

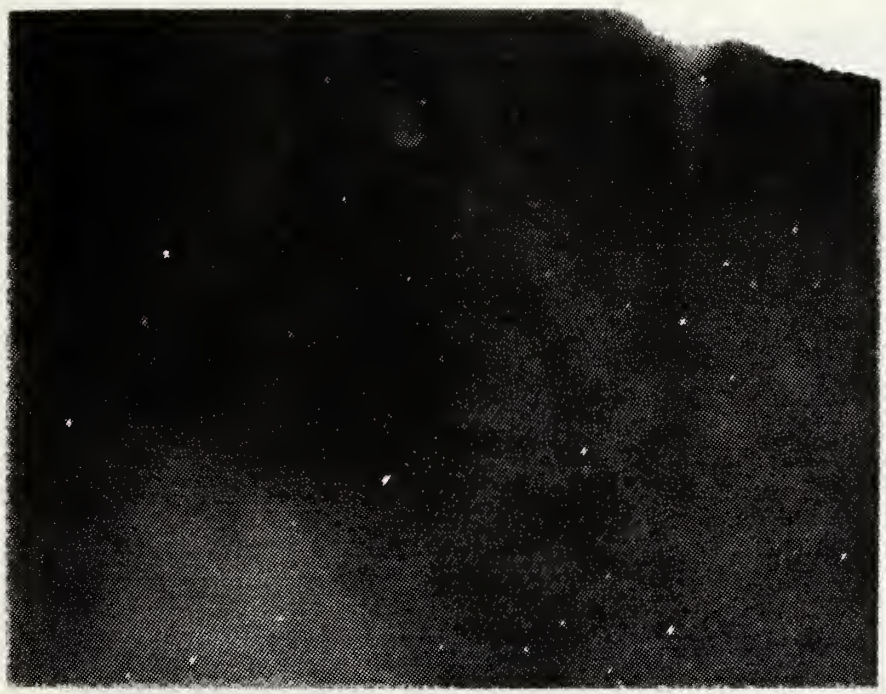

Figure 4.10 Undamaged Slide, Indirect Illumination Showing Surface Defects (800X Optical).

Figure 4.11 Large Micropit Damage Area (400X Optical).

Figure 4.12 Micropit Damage Area (800X Optical).

5. Micropitting

Figures 4.6 and 4.7 show close-ups of the ring area of one slide where small pits have formed. In Figure 4.6 the pit is in the middle of the ring and in Figure 4.7 it is at the inner edge of the ring.

Figure 4.8 is a photograph of the micropit at the middle ring area of Figure 4.6 . The pit is slightly oval of length 6.0 microns, width 4.5 microns and depth about 2.0 microns. There is a circular ring of diameter about 14 microns surrounding the pit. Apparently this is a site of microplasma production, where the plasma has formed from material ejected from the pit area and expanded to form the ring by condensation analogous to the large ring formation of Figure 4.4 . Figure 4.9 is a close-up of the pit showing the area of damage.

Metal particle inclusions in glass have been shown to be spots of increased thermal stress due to heating and expansion of the particle and subsequent breakdown of the material. Also, cracks or micropores in the glass are centers of local increased electric fields and subsequent increased damage probabilities. Figure 4.10 is a photo of an undamaged clean slide illuminated indirectly at total internal reflection showing surface scratches and defects that exist in all such slides. These defects are areas of increased damage probability due to the enhanced formation of standing waves that increase the local electric fields. The glass used as targets here is known to contain iron particles (about 0.03% by mole percent) which could certainly have effected the damage of Figure 4.8 or possibly a small defect in the glass at this point is responsible.

Figure 4.11 is another pit at the edge of the ring structure of the sample. It is larger and more noticably oval than the pit of Figure 4.8 having length 17.5 microns

and width 10.0 microns. Several smaller pits are seen nearby and an area of damage extends from the pit away from the laser impact area (in the direction of plasma expansion). Figure 4.12 shows another micropit formation area near the ring structure of a different target. These pits are seen to occur in a series of lines which lie perpendicular to the direction of plasma expansion along the plasma front. The fact that so many pits occur in a small region leads to the conclusion that the glass in this area must have contained surface defects that created "hot spots" where the hot plasma came in contact with them. Microplasmas were formed about these spots and the pits were created from the plasma formation and mini-explosion accompanying the high field intensities.

B. UNIPOLAR ARCING

Figure 4.14 is a scanning electron micrograph of an area near the edge of the ring structure of a target slide. This photograph shows many small holes about 1 micron or smaller in diameter that are possibly unipolar arc craters. The crater density is about $10^8/cm^2$. These holes have been observed in a great number of the target slides always near the inside edge of the ring structure. The size of the holes varies considerably with the largest visible in the upper left corner of Figure 4.14 at a diameter of 1.0 microns. The outline of the holes is fuzzy preventing a more useful interpretation of the picture. This fuzziness was apparent at high magnifications of the SEM primarily because of the poor conducting qualities of even the coated slides. However, it appears possible that each hole may have a rim which is characteristic of unipolar arc craters in conductors. The fact that the holes are small agrees with the theory addressed in Chapter II that, in order for

arcing to occur in poor conductors, the radially inward surface return current must converge to a smaller cathode spot.

Figure 4.15 is a further magnified view of a different group of arc holes. The center hole is much larger than the smaller surrounding holes and is not circular but ovally shaped. The center hole is about 1.6 microns long and about 0.8 microns wide while the surrounding holes have average diameter of about 0.3 microns.

Figure 4.13 is an optical microscope view at highest magnification of apparent craters. The craters are grouped at the center of the photo. Dust and interference patterns account for the poor quality of the picture. The holes appear to be of various sizes that average about 1.0 microns or less. These correlate roughly with the holes of Figure 4.14 .

Comparison of craters found in laser damaged conducting materials with the holes of Figures 4.14 through 4.13 is difficult for various reasons. Views of arc craters in conducting materials were seen at lower magnifications of the SEM and thus were easier to obtain. The craters here were not visible at magnifications less than about 800X. Before specific conclusions can be made concerning these holes, more research needs to be done in this area.

Figure 4.13 Craters Observed in Optical Microscope at Highest Magnification (800X Optical).

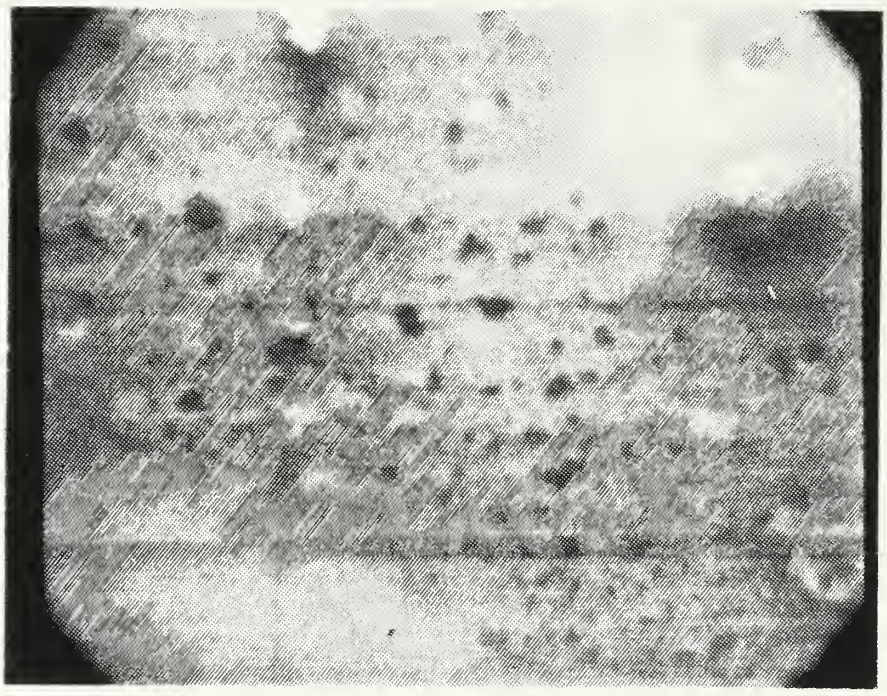

Figure 4.14 Craters at Inner Ring Area (5000X SEM).

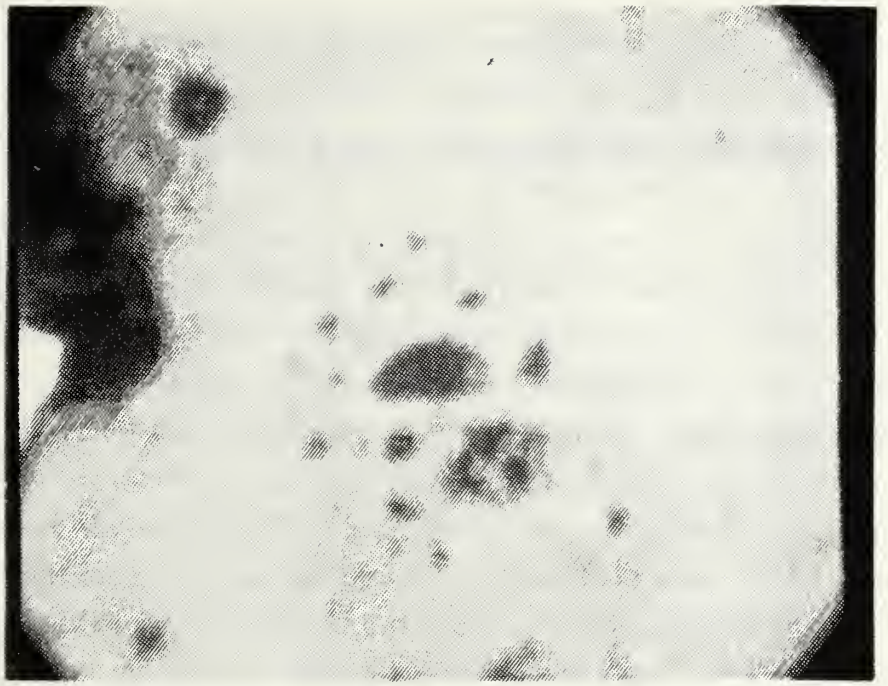

Figure 4.15 Possible Unipolar Arc Craters (10,000X SEM).

V. SUMMARY, CONCLUSIONS, AND RECOMMENDATIONS

The problem of laser-induced plasma surface damage in glass is a complex and fascinating one. So many variables are involved in some way in the damage process that, even under the most controlled experimental conditions, it is sometimes impossible to limit investigation of damage to one mechanism. In the final analysis, as is the case in so many endeavors, it is the interaction of particles on the atomic level that must be examined to fully understand the process.

The energy transfer process induced by a high power laser striking a glass target begins by evaporation and ionization of particles at or near the surface to form a hot plasma. At the high energy densities achieved in these experiments, the plasma can reach temperatures greater than 10^4K as it expands and begins to interact with the entrance surface. The plasma continues to be heated by the remainder of the laser pulse on the entrance surface while shielding the impact area of the target from the laser pulse if high enough plasma densities are obtained initially. Thermal stress from the hot plasma can crack and warp the surface. This heating of the surface by the plasma can cause pitting at particle inclusion areas where the stress of the particle against the glass can be greater than the fracture strength of the glass. Microcracks or pores can create pockets of high amplitude standing waves which increase damage probabilities in areas reached by the pulse. The cooling of the plasma upon expansion finally leads to deposition of the plasma particles on the glass in ring formations.

On the exit surface, high density plasma formation can create high amplitude standing waves at or just inside the surface that lead in some cases to micro-explosions that

create large holes in the exit surface. The exit surface is also susceptible to other forms of damage seen on the entrance surface except possibly for thermal stress because of the energy absorption that takes place in the glass and the entrance plasma.

Small holes found in most targets near the ring formations indicate the possible occurrence of unipolar arcing as a damage mechanism. High plasma temperatures ultimately are needed for unipolar arcing to occur. The return current that closes the current loop to maintain plasma quasineutrality can occur if the surface of the glass has been heated enough by the plasma to increase its electrical conductivity sufficiently. In the laser impact area, melting and thermal upheaval of the surface at these high energy densities would hide any unipolar arcing that might have occurred there.

Although further study of the unipolar arcing phenomenon in glass is needed, it is not unreasonable to conclude that unipolar arcing exists to some degree and may be significant. To what degree and how serious a problem it may be is a matter for further study. The other damage mechanisms investigated are real and pose a great problem to glass manufacturers and also to future weapons designers as laser weapons become widespread. Although transparent, glass absorbs about 8% of all radiation that impinges on it. As seen in this thesis, this figure can become higher as plasma formation increases the absorption at the surface.

Unipolar arcing in non-conducting materials needs to be studied further. Possible future experiments could examine lower energy densities nearer threshold for arcing damage. More refined techniques especially in the use of the SEM with non-conducting materials are needed. A high quality glass polished to eliminate most surface defects and manufactured carefully to eliminate metal inclusions could be

obtained and used for targets. Carefully controlled experiments such as these could aid considerably in increasing understanding of this topic.

LIST OF REFERENCES

1. Dupont, H., Donzel, A., and Ernest, J., "On Laser-Induced Breakdown and Fracture in Glasses", Applied Physics Letters, Vol. 11, No. 9, 1967, pp. 271 - 272

2. Boling, N. L., Crisp, M. D., and Dube, G., "Laser Induced Surface Damage", Applied Optics, Vol. 12, No. 4, April 1973, p. 650

3. Swain, J. E., "Surface Damage Threshold Measurements for Several Laser Glasses", Damage in Laser Glass, ASTM STP 469, American Society for Testing and Materials, 1969, pp. 69-78

4. Owens-Illinois Technical Center Report ARPA 1441, Damage Threshold Studies of Glass Laser Materials by N. L. Boling, pp. 3-9, 30 June 1972

5. Owens-Illinois Technical Center Report ARPA 2050, Damage Threshold Studies of Glass Laser Materials by N. L. Boling and G. Dube, p. 25, 30 June 1973

6. Hopper, R. W., Lee, C., and Uhlmann, D. R., The Inclusion Problem in Laser Glass, paper presented at the Symposium on Damage in Laser Materials, 2nd, Boulder, Colorado, 24 - 25 June 1970, p.55

7. Crisp, M. D., Boling, N. L., and Dube, G., "Importance of Fresnel Reflections in Laser Surface Damage of Transparent Dielectrics", Applied Physics Letters, Vol. 21, No. 8, pp. 364-366, 15 October 1972

8. Jacobson, J. F., Examination of Laser-Produced Pressure Pulses in a Gallium Arsenide Solar Cell, M. S. Thesis, Naval Postgraduate School, Monterey, California, June 1976

9. Bliss, E. S., "Laser Damage Mechanisms in Transparent Dielectrics", Damage in Laser Glass ASTM 469, American Society for Testing and Materials, 1969, pp. 9-13

10. Bloembergen, N., "Roles of Cracks, Pores, and Absorbing Inclusions on Laser Induced Damage Threshold at Surfaces of Transparent Dielectrics", Applied Optics, Vol. 12, No. 4, April 1973, p. 661

11. Hopper, R. W., and Uhlmann, D. R., "Mechanism of Inclusion Damage in Laser Glass", Journal of Applied Physics, Vol. 41, No. 10, September 1970, p. 4023

12. Bennett, H. S., "Absorbing Centers in Laser Glasses", Damage in Laser Materials NBS 341, edited by A. J. Glass and A. H. Guenther, National Bureau of Standards, June 1970, p. 51

13. Schwirzke, F. R., "Laser Induced Unipolar Arcing", Laser Interaction and Related Phenomena, Vol. 6, edited by Heinrich Hora and George H. Miley, Plenum Publishing Corporation, 1984, p. 351

14. Ryan, F. T. and Shedd, S. T., A Study of the Unipolar Arcing Damage Mechanism on Selected Conductors and Semiconductors, M. S. Thesis, Naval Postgraduate School, Monterey, California, June 1981, pp. 12-19

15. Naval Postgraduate School Report NPS-61-83-008, Unipolar Arcing, A Basic Laser Damage Mechanism by F. R. Schwirzke, 5 May 1983, pp. 1-2

16. Davis, L. J., Self-Generated Magnetic Fields Produced by Laser Bombardment of a Solid Target, M. S. Thesis, Naval Postgraduate School, Monterey, California, 1971, pp. 14 - 30

17. Corning Glass Works, Corning, New York, Properties of Selected Commercial Glasses, pp. 3 - 9, 1961

18. Schadegg, Lawrence M., The Dynamics of a Laser Produced Heavy Ion Plasma, M. S. Thesis, Naval Postgraduate School, Monterey, California, June 1970, p. 8

19. Corporate Technology Division, Owens-Illinois, Inc., Final Technical Report, 31 August 1974, Damage Threshold Studies of Glass Laser Materials by N. L. Boling and G. Dube, pp. 31-32

20. McKee, L. L., III, An Investigation of the Self-Generated Magnetic Fields Associated with a Laser-Produced Plasma, Ph.D. Dissertation, Naval Postgraduate School, Monterey, California, December 1972, p. 65

BIBLIOGRAPHY

Barker, J. H. and Rush, R. J., An Investigation of Plasma-Surface Interactions on Selected Conductors and Insulators, M. S. Thesis, Naval Postgraduate School, Monterey, California, December, 1980

Chen, F. F., Introduction to Plasma Physics and Controlled Fusion, Vol. 1: Plasma Physics, Plenum Press, 1984

Hecht, E. and Zajac, A., Optics, Addison-Wesley, 1979

Hoover, T. J., An Investigation of Unipolar Arcing in Various Conductors and Metallic Glasses, M. S. Thesis, Naval Postgraduate School, Monterey, California, September 1981

Naval Postgraduate School Report NPS-61-84-004, Short Pulse Laser and Plasma Surface Interactions by F. W. Schwirtzke, 2 April 1984

Verdeyen, J. T., Laser Electronics, Prentice Hall, 1981

Yariv, A., Optical Electronics, Third Edition, Holt, Rinehart, and Winston, 1985

INITIAL DISTRIBUTION LIST

		No. Copies
1.	Defense Technical Information Center Cameron Station Alexandria, Virginia 22304-6145	2
2.	Library, Code 0142 Naval Postgraduate School Monterey, California 93943-5100	2
3.	Lieutenant Commander Richard D. Uyak 281 N. Winding Way Merion, Pennsylvania 19066	1
4.	Professor F. Schwirzke Department of Physics, Code 61Sw Naval Postgraduate School Monterey, California 93943-5100	2

215635

Thesis
U93 Uyak
c.1 An investigation of laser induced surface damage in glass.